



Shift from androgen to estrogen action causes abdominal muscle fibrosis, atrophy, and inguinal hernia in a transgenic male mouse model

Hong Zhao^a, Ling Zhou^a, Lin Li^b, John Coon V^a, Robert T. Chatterton^a, David C. Brooks^a, Enze Jiang^a, Li Liu^c, Xia Xu^d, Zhiyong Dong^a, Francesco J. DeMayo^e, Jonah J. Stulberg^f, Warren G. Tourtellotte^b, and Serdar E. Bulun^{a,1}

^aDepartment of Obstetrics and Gynecology, Division of Reproductive Science in Medicine, Feinberg School of Medicine, Northwestern University, Chicago, IL 60611; ^bDepartment of Pathology, Division of Neuropathology, Feinberg School of Medicine, Northwestern University, Chicago, IL 60611; ^cDepartment of Geriatrics, First Affiliated Hospital of Nanjing Medical University, Nanjing, Jiangsu 210029, China; ^dLaboratory of Proteomics and Analytical Technologies, SAIC-Frederick, National Cancer Institute, National Institutes of Health, Frederick, MD 21702; ^eReproductive and Developmental Biology Laboratory, National Institute of Environmental Health Sciences, National Institutes of Health, Durham, NC 27709; and ^fDepartment of Surgery, Gastrointestinal/Endocrine Division, Feinberg School of Medicine, Northwestern University, Chicago, IL 60611

Edited by Bert W. O'Malley, Baylor College of Medicine, Houston, TX, and approved September 25, 2018 (received for review June 1, 2018)

Inguinal hernia develops primarily in elderly men, and more than one in four men will undergo inguinal hernia repair during their lifetime. However, the underlying mechanisms behind hernia formation remain unknown. It is known that testosterone and estradiol can regulate skeletal muscle mass. We herein demonstrate that the conversion of testosterone to estradiol by the aromatase enzyme in lower abdominal muscle (LAM) tissue causes intense fibrosis, leading to muscle atrophy and inguinal hernia; an aromatase inhibitor entirely prevents this phenotype. LAM tissue is uniquely sensitive to estradiol because it expresses very high levels of estrogen receptor- α . Estradiol acts via estrogen receptor- α in LAM fibroblasts to activate pathways for proliferation and fibrosis that replaces atrophied myocytes, resulting in hernia formation. This is accompanied by decreased serum testosterone and decreased expression of the androgen receptor target genes in LAM tissue. These findings provide a mechanism for LAM tissue fibrosis and atrophy and suggest potential roles of future nonsurgical and preventive approaches in a subset of elderly men with a predisposition for hernia development.

aromatase | estrogen receptor- α | androgen | fibrosis | hernia

Inguinal hernia is a common malady in elderly men, and hernia repair is the most commonly performed general surgical procedure in the United States. Although its pathogenesis is poorly understood, the lifetime risk of inguinal hernia is 27% in men and 3% in women (1). Approximately 800,000 inguinal hernia repairs are performed every year (1, 2), and annual health care costs directly attributable to inguinal hernia exceed \$2.5 billion in the United States (3). Surgery is the only treatment option for an inguinal hernia. Unfortunately, complications, such as long-term postoperative pain, nerve injury, wound infection, and recurrence continue to challenge surgeons and patients (4–7). There are no actively utilized animal models for studying inguinal hernia or sex steroid-related muscle fibrosis and atrophy; furthermore, currently there are no experimental or approved medical options for the prevention of inguinal hernias in subsets of elderly men.

Inguinal hernias are termed “indirect” if the bowel is herniated via a defective inguinal ring or “direct” if the bowel protrudes through another weakened portion of lower abdominal muscle (LAM) wall (3, 5). The inguinal canal in male mice, which connects the abdominal cavity and the scrotum, is structurally similar to that in men and particularly vulnerable to indirect herniation of bowel (8). Therefore, experimental scrotal hernias in mice have similarities to indirect inguinal hernia in humans, which comprise two-thirds of all inguinal hernias in men (5). Previous studies in mice suggest that the development of scrotal hernias may be associated with abnormalities in the

abdominal muscles, particularly those in the inguinal region (9, 10). In men, histological studies have identified myocyte (myofiber) atrophy, fibrosis, and fatty degeneration in the internal inguinal ring area from indirect hernia patients and in the abdominal wall surrounding a direct hernia border (11–13). LAM tissue is composed of layers of oblique and transverse skeletal muscle made of myocytes. Stromal tissue, a mixture of well-organized fibroblasts and extracellular matrix (ECM), surrounds a single myocyte, fascicles (groups of myocytes), or the entire muscle tissue (groups of fascicles), and eventually becomes the deep fascia. An inguinal hernia occurs if both the muscle and adjacent fascia are weakened and can no longer support bowel in the abdomen.

Age is a significant risk factor for inguinal hernia formation in men with a striking increase in incidence after the age of 55 y. By the time they reach 75 y of age, nearly 50% of men will develop inguinal hernia (14, 15). Indirect inguinal hernia, which comprises 70% of all hernias, peaks between the ages of 70 and 79 y in men (16). It is a disease of primarily elderly men. The increased risk of inguinal hernia in elderly men may be related to age-linked skeletal muscle atrophy associated with fibrosis in the inguinal area. However, the mechanisms mediating skeletal

Significance

Inguinal hernia is one of the most common disorders that affect elderly men. A major pathology underlying inguinal hernia is the fibrosis and other degenerative changes that affect the lower abdominal muscle strength adjacent to the inguinal canal. Here we describe a critical role of estrogen and its nuclear receptor that enhance fibroblast proliferation and muscle atrophy, leading to inguinal hernia. Further research may reveal a potential role of estrogen ablation to prevent muscle fibrosis or hernia in a subset of elderly men.

Author contributions: H.Z., F.J.D., W.G.T., and S.E.B. designed research; H.Z., L.Z., L. Li, J.C., R.T.C., D.C.B., E.J., and X.X. performed research; H.Z. and L. Li contributed new reagents/analytic tools; L. Liu collected the human muscle samples; H.Z., L.Z., L. Liu, Z.D., J.J.S., and S.E.B. analyzed data; and H.Z. and S.E.B. wrote the paper.

The authors declare no conflict of interest.

This article is a PNAS Direct Submission.

This open access article is distributed under [Creative Commons Attribution-NonCommercial-NoDerivatives License 4.0 \(CC BY-NC-ND\)](https://creativecommons.org/licenses/by-nc-nd/4.0/).

Data deposition: The data reported in this paper have been deposited in the Gene Expression Omnibus (GEO) database, <https://www.ncbi.nlm.nih.gov/geo/> (accession no. GSE92748).

¹To whom correspondence should be addressed. Email: s-bulun@northwestern.edu.

This article contains supporting information online at www.pnas.org/lookup/suppl/doi:10.1073/pnas.1807765115/-DCSupplemental.

Published online October 16, 2018.

muscle atrophy and fibrosis that increases the risk of hernia formation are not well understood.

Sex steroid hormones change as men age. Age-related changes in serum estradiol (E_2) levels in men are conflicting, as some studies have reported increases but others have noted unchanged or even decreased E_2 levels with advancing age (17–24). Conversion of circulating testosterone (T) to E_2 via aromatase expression in bulky tissues—namely, skeletal muscle and adipose tissue—produces the majority of estrogen in men (25, 26). Human muscle and adipose tissue aromatase expression or activity has been found to increase with advancing age, which coincides with the incidence of inguinal hernia (25, 27–29). In the 1930s, two separate laboratories reported that ~40% of male mice that received postnatal estrogen injections or ovarian grafts developed scrotal hernias (8, 30). Estrogen injections initiated as early as postnatal day 28 or as late as 30 wk of age led to the development of scrotal hernia within a few weeks (8). These data were suggestive of a direct link between local tissue estrogen and acquired inguinal hernias and do not support the possible contribution of a congenital defect. The underlying cellular and molecular mechanisms, however, remain unknown. Conversely, serum T levels decrease by 20% by age 50 and by 50% by age 80 y in association with decreased skeletal muscle mass in men (31–33). A higher ratio of E_2 to T was observed in elderly men compared with younger men (31). It remains unclear whether the age-related shift in the estrogen to T ratio in the LAM tissue causes muscle fibrosis and atrophy and predisposes a subset of older men to develop inguinal hernia.

Aromatase is the only enzyme that catalyzes the conversion of T to E_2 . The tissue distribution patterns of aromatase expression in humans and mice are markedly distinct. In male mice, aromatase is expressed only in the testes, gonadal fat, and brain via 3 promoters, whereas humans use 10 distinct promoters to express aromatase in many peripheral tissues, including skeletal muscle. We recently generated mice expressing aromatase from the human promoter (*Arom^{hum}*) to mimic human physiology with respect to aromatase expression and estrogen production (34). *Arom^{hum}* mice physiologically express the human aromatase gene in many peripheral tissues, including skeletal muscle (25, 35, 36). Intriguingly, male *Arom^{hum}* mice exhibit increased estrogen levels in peripheral LAM tissues, low serum T levels, and scrotal hernia formation, mimicking what has been observed in a subset of older men. Thus, we used this mouse model to test the hypothesis that alterations in E_2 , T, and their nuclear receptors, estrogen receptor- α (ER α) and androgen receptor (AR), in LAM tissues lead to fibrosis, skeletal muscle atrophy, and the development of scrotal hernias. We also investigated some of the underlying cellular and molecular mechanisms behind hernia formation.

Results

Humanized Aromatase Expression and Physiological Estrogen Production in LAM Tissues Are Associated with Scrotal Hernia Formation in *Arom^{hum}* Mice. *Arom^{hum}* mice were generated and characterized as previously described (34). Briefly, we isolated a human BAC clone containing the human aromatase coding sequence flanked by its full-length 93-kb 5'-regulatory region and the 3'-polyadenylation site, and injected the BAC clone DNA into pronuclear mouse embryos to generate transgenic mice with a single copy of the transgene in the germline. We obtained six male transgene-positive founders in two independent male transgenic lines, F1771 and F1772. The *Arom^{hum}* F1771 line included a >78-kb 5'-flanking region encompassing the distal promoters I.4, I.7, I.f, as well as the proximal cluster of promoters I.6 and I.3/PII (Fig. 1A), whereas the *Arom^{hum}* F1772 line had a 4.3-kb 5'-flanking region containing only the proximal promoters I.6 and I.3/PII (34). Bilateral scrotal hernias were observed in 90–100% of male *Arom^{hum}* mice by 12 wk from all two lines established from the founders, whereas none of the WT

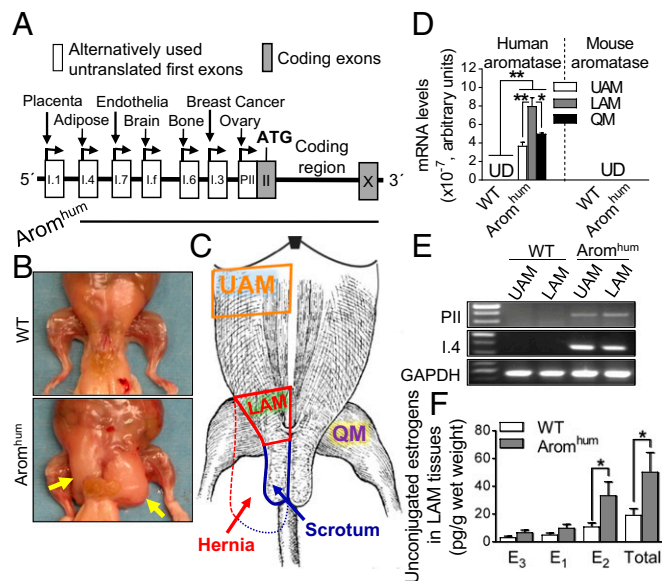


Fig. 1. Human aromatase expression, abdominal muscle tissue estrogen levels, and scrotal hernia formation in *Arom^{hum}* transgenic mice. (A) Schematic of the human BAC clone construct used to generate *Arom^{hum}* transgenic mice, which contained all alternatively used promoters with downstream first exons of the aromatase gene except for placental exon I.1. (B) Dissected abdominal musculature of 26-wk-old WT and *Arom^{hum}* mice. Yellow arrows indicate scrotal hernia. (C) Schematic of mouse abdominal muscle anatomy in WT and *Arom^{hum}* mice. UAM, LAM, QM, the scrotum, and hernia are shown in the sketch. Solid red line and solid blue line indicate normal LAM tissue and normal scrotum in WT mice, respectively. Dashed red line indicates expanded fibrotic LAM tissue that comprises the hernia wall contiguous with the scrotum (dashed blue line) in *Arom^{hum}* mice. (D) Human and mouse aromatase mRNA levels were determined in UAM, LAM, and QM of *Arom^{hum}* mice. UD, undetermined. Statistical analysis by two-way ANOVA with Sidak's multiple comparison test, * $P < 0.05$, ** $P < 0.01$, $n = 8$ mice per group. (E) Exon-specific RT-PCR confirmed that distinct promoters drive human aromatase expression in the abdominal muscle tissues of *Arom^{hum}* mice. GAPDH mRNA levels served as internal control. Data are representative of three independent experiments. (F) LAM tissue unconjugated estrogens were measured by LC-MS² assay. E₁, E₂, and E₃ are shown. Two-tailed Student's t test, * $P < 0.05$, $n = 14$ mice.

animals developed any hernias. Because all founder lines showed a similar phenotype, we primarily reported the results obtained from a single founder from the *Arom^{hum}* F1771 line (referred to as *Arom^{hum}* in this report). The scrotal hernia sacs contained abdominal viscera, including gonads, gonadal fat, urinary bladder, and bowel (Fig. 1B). In *Arom^{hum}* mice, LAM tissues became progressively fibrotic and distended, comprising the major part of the hernia wall, contiguous with the scrotum (Figs. 1C and 2C and D). Human aromatase expression driven by its native promoters in *Arom^{hum}* mice resembled the human pattern of aromatase expression (SI Appendix, Table S1) (25, 35–37).

Because inguinal hernia is associated with fibrosis of the LAM tissue, we analyzed the expression and promoter usage of aromatase and estrogen formation in the abdominal muscle tissue of *Arom^{hum}* mice. We demonstrated that human aromatase mRNA but not mouse aromatase mRNA was readily detectable in LAM tissue, upper abdominal muscle (UAM) tissue, and quadriceps muscle (QM) tissue of *Arom^{hum}* mice, whereas both human and mouse aromatase mRNA was absent in these muscle tissues in WT mice (Fig. 1D). 5'-RACE showed that aromatase mRNA was transcribed primarily from promoter I.4 of the human aromatase gene in abdominal muscle and QM tissues of *Arom^{hum}* mice (SI Appendix, Table S1). Additionally, exon-specific RT-PCR showed that human aromatase expression was driven primarily

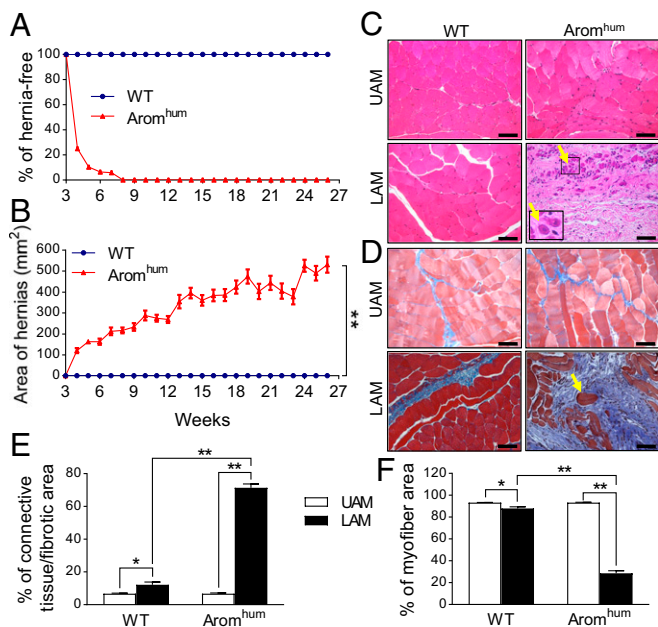


Fig. 2. Human aromatase expression and estrogen production lead to LAM tissue fibrosis, myocyte atrophy, and the development of scrotal hernia in *Arom^{hum}* mice. (A) The incidence of scrotal hernia. Scrotal hernia formation was monitored by weekly visual inspection from 3 to 26 wk of age. No scrotal hernia was seen in the WT group. $n = 32$ mice. (B) The area of scrotal hernia was measured from 3- to 26-wk-old mice. Two-tailed Student's t test, $**P < 0.01$ for *Arom^{hum}* vs. WT, $n = 32$ mice. (C) H&E and (D) Masson's trichrome staining of UAM and LAM from 26-wk-old WT and *Arom^{hum}* mice. $n = 10$ mice for C and D. Yellow arrows in C and D indicate one of many atrophied myocytes. (Scale bars, 100 μm ; Magnification: *Inset* in C, 40 \times .) Quantification of the percentage of connective tissue or fibrotic area (E) or myofiber area (F) in WT and *Arom^{hum}* mice. Ten representative high-power fields were analyzed in each tissue. Two-way ANOVA with Tukey's multiple comparison test, $*P < 0.05$, $**P < 0.01$, $n = 8$ mice per group.

by promoters I.4 and to a lesser extent PII in abdominal muscle tissues of *Arom^{hum}* mice (Fig. 1E). The aromatase mRNA expression profile and promoter usage in other tissues of male *Arom^{hum}* mice are summarized in *SI Appendix, Table S1*. Thus, human aromatase expression is driven by its native promoters in a wide variety of male *Arom^{hum}* mouse tissues, including skeletal muscle (25, 35–37).

To determine whether humanized aromatase expression in the *Arom^{hum}* mouse extragonadal tissue, including abdominal muscle, is accompanied by a change in tissue estrogen levels and circulating hormone levels, we measured tissue concentrations of estrogens [estrone (E_1), E_2 , and estriol (E_3)] using liquid chromatography-tandem mass spectrometry (LC-MS²) (Fig. 1F), and also compared peripheral serum levels of E_2 and the gonadotropins luteinizing hormone (LH) and follicle-stimulating hormone (FSH) using LC-MS² and radioimmunoassay (*SI Appendix, Fig. S1*). Compared with WT mice, total estrogen levels in LAM tissues were significantly higher by 2.6-fold in *Arom^{hum}* mice. Most importantly, LAM tissue levels of the biologically potent estrogen, E_2 , were 3.1-fold higher in *Arom^{hum}* mice compared with WT littermates (Fig. 1F). However, serum E_2 levels measured by LC-MS² were not significantly different between WT and *Arom^{hum}* males (Fig. 3C and *SI Appendix, Fig. S1A*). Serum FSH concentrations were significantly lower in *Arom^{hum}* mice (64%) compared with WT mice. Decreased FSH levels in the *Arom^{hum}* mice may be due to increased E_2 production via human aromatase expression in hypothalamic tissue (*SI Appendix, Table S1*). Serum LH concentrations were lower but did not reach significance in *Arom^{hum}* mice compared with

WT littermates. These results show that local LAM tissue E_2 levels, but not circulating E_2 levels, led to hernia formation in male *Arom^{hum}* mice.

The Development of Scrotal Hernias Is Associated with Fibrosis and Myocyte Atrophy in LAM Tissue of *Arom^{hum}* Mice. We studied WT and *Arom^{hum}* mice from 1 to 26 wk of age for the development of hernias. Minimal lower abdominal bulging was first observed in 75% of *Arom^{hum}* mice at 4 wk, with noticeable bulging by 8 wk in all *Arom^{hum}* mice, followed by frank scrotal herniation by 12 wk in all *Arom^{hum}* mice (Fig. 2A). Hernia size continued to increase during the whole observation period (up to 26 wk of age) (Fig. 2B).

We also studied the effects of muscle aromatase expression and estrogen production on skeletal muscle histology. UAM and QM did not show any major structural differences between WT and the *Arom^{hum}* mice (Fig. 2C and *SI Appendix, Fig. S4*), while the morphology of extended LAM tissue that comprises the major part of hernia wall was markedly altered in *Arom^{hum}* mice (Fig. 1B and C). At 24 wk, LAM tissue of *Arom^{hum}* mice showed a marked decrease in myocyte size and centralized nuclei, indicating myocyte atrophy (Fig. 2C, yellow arrow, *Inset*). Masson's trichrome staining of LAM sections showed a marked increase in collagen deposition in the context of myocyte atrophy in *Arom^{hum}* mice compared with WT mice (Fig. 2D–F). Together, these results clearly indicate that hernia formation induced by LAM E_2

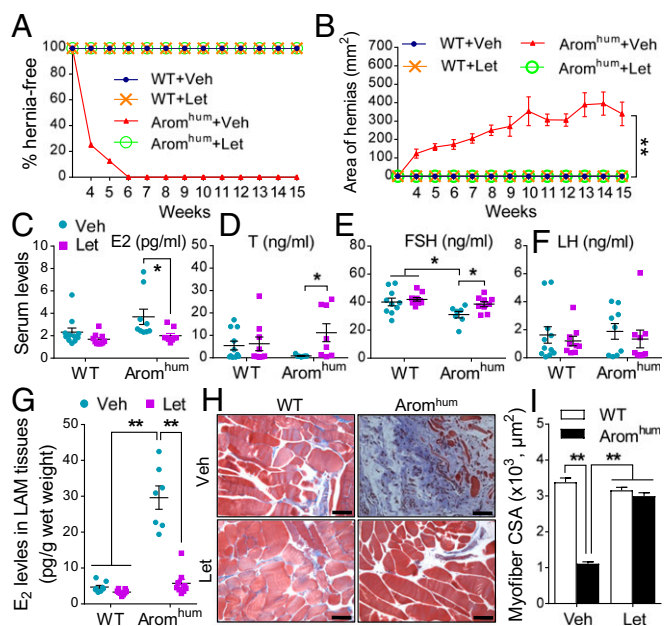


Fig. 3. Aromatase inhibitor rescues LAM tissue fibrosis and myocyte atrophy and prevents the development of scrotal hernias in *Arom^{hum}* mice. Three-week-old mice were treated with vehicle (Veh) or letrozole (Let) for 12 wk. (A) The incidence of scrotal hernia in *Arom^{hum}* mice. (B) The area of scrotal hernia in *Arom^{hum}* mice. Two-tailed Student's t test, $**P < 0.01$. Serum E_2 (C), T (D), FSH (E), and LH (F) were measured in WT and *Arom^{hum}* mice after Veh or Let treatment. Statistical analysis by two-way ANOVA with Sidak's multiple comparison test, $*P < 0.05$. (G) E_2 levels in LAM tissue. Statistical analysis by two-way ANOVA with Tukey's multiple comparison test, $**P < 0.01$. Serum and LAM E_2 levels (C and G) were measured by LC-MS² assay. (H) Representative photomicrographs of Masson's trichrome-stained LAM sections of WT and *Arom^{hum}* mice. (Scale bars, 100 μm .) (I) Quantification of myofiber cross-sectional area (CSA) in WT and *Arom^{hum}* mice. A minimum of 1,000 cells in 10 different high-power fields were analyzed in each tissue. Two-way ANOVA with Tukey's multiple comparison test, $**P < 0.01$. $n = 10$ mice per group.

production is associated with LAM tissue fibrosis and myocyte atrophy.

Administration of an Aromatase Inhibitor Prevents Scrotal Hernia Development in *Arom^{hum}* Mice. Aromatase inhibitors represent the most effective endocrine treatment for postmenopausal breast cancer (34, 38). The role of aromatase inhibitors in prevention of scrotal hernias, however, is unknown. Here we investigated whether blockage of aromatase activity using a slow-release aromatase inhibitor pellet (letrozole, 10 μ g/d per mouse) can prevent scrotal hernia development in *Arom^{hum}* mice. Intriguingly, none of the *Arom^{hum}* mice administered subcutaneous letrozole at 3 wk of age developed scrotal hernia until the end of treatment (15 wk of age) (Fig. 3*A* and *B*). Serum E_2 levels were not significantly different between WT and *Arom^{hum}* mice, but they significantly decreased in *Arom^{hum}* mice after letrozole treatment (Fig. 3*C*). T levels in vehicle-treated *Arom^{hum}* mice were lower compared with WT mice and were increased by levels comparable to those in WT mice after letrozole treatment (Fig. 3*D*). Similarly, FSH levels in vehicle-treated *Arom^{hum}* mice were significantly lower compared with WT mice and increased to normal (WT) levels with letrozole treatment (Fig. 3*E*). However, letrozole treatment did not change serum LH levels in either WT or *Arom^{hum}* mice, nor did it change serum E_2 , T, or FSH levels in WT mice (Fig. 3*C–F*). Most importantly, LAM tissue E_2 levels were 6.3-fold higher in *Arom^{hum}* mice compared with WT littermates and letrozole treatment completely restored LAM E_2 levels to normal (WT) levels (Fig. 3*G*). Development of fibrosis in the LAM tissue of *Arom^{hum}* mice was completely prevented with letrozole treatment (Fig. 3*H*). The myofiber cross-sectional area in untreated *Arom^{hum}* mice was significantly smaller than in WT mice, indicating muscle atrophy. Letrozole treatment completely prevented myofiber atrophy in *Arom^{hum}* mice (Fig. 3*H* and *I*). These data demonstrate that aromatase inhibition via letrozole treatment can inhibit LAM aromatase activity, restore LAM tissue E_2 levels and serum T and FSH levels to normal levels, and prevent LAM tissue fibrosis, muscle atrophy, and hernia formation.

Higher Estrogen Sensitivity in LAM Tissue Is Accounted for by High ER α Levels in Stromal Fibroblasts. E_2 exerts its biological effects by binding and signaling through at least three distinct receptors, ER α , ER β , and Gpr30 (39–41). The levels of ER α and ER β in different muscle groups are markedly different (42). In *Arom^{hum}* mice, ER β mRNA levels were significantly lower in LAM tissue compared with UAM tissue (SI Appendix, Fig. S2*A*). Moreover, ER α mRNA levels were 350- and 597-fold higher than ER β mRNA levels in UAM tissue and 610- and 1,786-fold higher than ER β mRNA levels in LAM tissue of WT and *Arom^{hum}* mice, respectively (SI Appendix, Fig. S2*B*). Additionally, although Gpr30 mRNA levels were significantly higher in LAM tissues than UAM tissues, ER α mRNA levels were 510- and 617-fold higher than Gpr30 mRNA levels in UAM tissue and 263- and 244-fold higher than Gpr30 mRNA levels in LAM tissue of WT and *Arom^{hum}* mice, respectively (SI Appendix, Fig. S2*C* and *D*). Most importantly, Gpr30 mRNA levels were significantly lower in LAM fibroblasts compared with UAM fibroblasts (SI Appendix, Fig. S2*E*). ER α mRNA levels were 47- and 54-fold higher than Gpr30 mRNA levels in UAM fibroblasts and 277- and 215-fold higher than Gpr30 mRNA levels in LAM fibroblasts of WT and *Arom^{hum}* mice, respectively (SI Appendix, Fig. S2*F*). Thus, ER α seems to be the predominant receptor that plays a key role in estrogen sensitivity and hernia formation in LAM tissue of *Arom^{hum}* mice. Furthermore, in muscle tissue, ER α mRNA levels were highest in LAM, modest in UAM, and lowest in QM in both WT and *Arom^{hum}* mice (Fig. 4*A*). ER α mRNA levels in LAM of all mice were significantly higher than those in UAM. QM ER α mRNA levels were significantly lower than UAM and

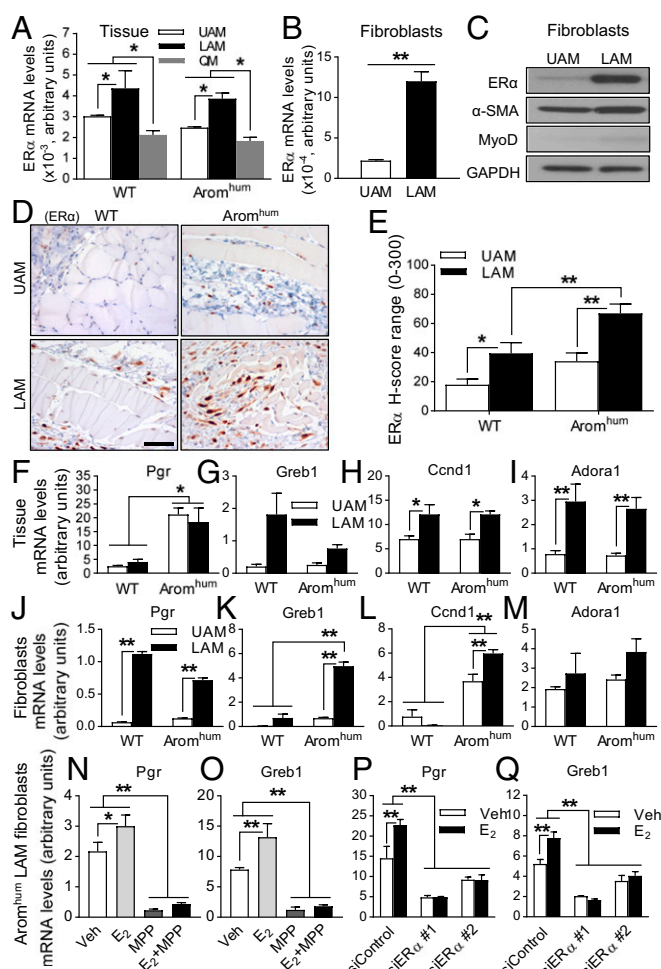


Fig. 4. ER α expression is higher in LAM tissue fibroblasts of both WT and *Arom^{hum}*, which contributes to the higher estrogen-responsive gene expression in LAM tissue of *Arom^{hum}* mice. (A) Relative mRNA levels of ER α in UAM, LAM, and QM of WT and *Arom^{hum}* mice. Two-way ANOVA with Tukey's multiple comparison test. * $P < 0.05$. $n = 10$ mice in each group. (B) ER α mRNA levels and (C) ER α protein levels in primary fibroblasts from UAM and LAM of WT mice. The data shown in C are representative of three independent experiments. Two-tailed Student's t test, *** $P < 0.01$, $n = 3$. (D) ER α localization in UAM and LAM of WT and *Arom^{hum}* mice was measured by IHC staining. (Scale bar, 50 μ m.) (E) A minimum of 1,000 nuclei were counted in sections to calculate the average H-score of ER α in fibroblasts of UAM and LAM from WT and *Arom^{hum}* mice. Two-way ANOVA with Sidak's multiple comparison test, * $P < 0.05$, ** $P < 0.01$, $n = 10$. mRNA levels of *Pgr*, *Greb1*, *Ccnd1*, and *Adora1* in tissue lysates (F, G, H, and I; $n = 9$) and primary fibroblasts (J, K, L, and M; $n = 6$) of UAM and LAM from WT and *Arom^{hum}* mice. mRNA levels of *Pgr* and *Greb1* in LAM primary fibroblasts from *Arom^{hum}* mice after MPP (10 μ M) treatment (N and O) or siRNA-mediated knockdown of ER α (P and Q) in the presence or absence of E_2 (10 nM). Cells were pretreated with MPP for 2 h before the addition of E_2 . Veh, vehicle. Two-way ANOVA with Sidak's multiple comparison test, * $P < 0.05$, ** $P < 0.01$. GAPDH mRNA or protein levels served as controls.

LAM in all mice. ER α protein levels tended to be higher but did not reach significance in LAM homogenates compared with UAM homogenates in either WT or *Arom^{hum}* mice (SI Appendix, Fig. S3).

Because muscle is a heterogeneous tissue consisting of myocytes, stromal cells (fibroblasts), vascular endothelial cells, and other cell types, it is possible that specific expression of ER α in a particular cell type may not be accurately assessed by analyzing whole-tissue homogenates. Thus, we isolated fibroblasts from

Table 1. Microarray analysis of LAM tissue in WT and *Arom^{hum}* mice

Gene symbol	Definition	Fold-change	Adjusted <i>P</i> value
Top 13 up-regulated fibrotic genes in LAM of <i>Arom^{hum}</i> mouse			
<i>Kiss1</i>	KISS-1 metastasis-suppressor	31.13	0.009
<i>Ren1</i>	Renin 1 structural	7.87	0.026
<i>Emb</i>	Embigin	5.20	0.020
<i>Krt8</i>	Keratin 8	4.38	0.005
<i>Timp1</i>	Tissue inhibitor of metalloproteinase 1, transcript variant 2	4.19	0.009
<i>Krt7</i>	Keratin 7	3.05	0.007
<i>Spon2</i>	Spondin 2, extracellular matrix protein	2.83	0.058
<i>Krt18</i>	Keratin 18	2.71	0.013
<i>Spon1</i>	Spondin 1, (f-spondin) extracellular matrix protein	2.54	0.009
<i>Tnc</i>	Tenascin C	2.52	0.079
<i>Plod2</i>	Procollagen lysine, 2-oxoglutarate 5-dioxygenase 2	2.42	0.018
<i>Eln</i>	Elastin	2.38	0.020
<i>Col8a1</i>	Collagen, type VIII, α 1	2.21	0.040
Top 8 down-regulated androgen responsive genes in LAM of <i>Arom^{hum}</i> mouse			
<i>Amd2</i>	S-adenosylmethionine decarboxylase 2	3.43	0.036
<i>Cyp2e1</i>	Cytochrome P450, family 2, subfamily e, polypeptide 1	3.22	0.045
<i>Cpeb4</i>	Cytoplasmic polyadenylation element binding protein 4	1.89	0.025
<i>Idh3g</i>	Isocitrate dehydrogenase 3 (NAD ⁺), γ	1.85	0.015
<i>Tiam1</i>	T cell lymphoma invasion and metastasis 1	1.77	0.037
<i>Cntnap2</i>	Contactin associated protein-like 2	1.75	0.043
<i>Tst</i>	Thiosulfate sulfurtransferase, mitochondrial	1.75	0.037
<i>Hrasls</i>	HRA5-like suppressor	1.73	0.043

Fibrotic genes were up-regulated and androgen-responsive genes were down-regulated in *Arom^{hum}* mice vs. WT mice.

UAM and LAM tissues of WT mice and found that mRNA and protein levels of ER α were markedly higher in LAM fibroblasts than UAM fibroblasts (Fig. 4 B and C). Primary fibroblast specificity was confirmed by the presence of a fibroblast marker (α -SMA) and the absence of a myocyte marker (MyoD). We used immunohistochemistry (IHC) to further confirm ER α protein levels in LAM fibroblasts of WT and *Arom^{hum}* mice. ER α immunoreactivity was almost exclusively observed in the stromal fibroblasts, but rarely present in myocytes (Fig. 4D and *SI Appendix, Fig. S4*). The H-score of ER α ⁺ stromal cells was significantly higher in LAM tissue than in UAM tissue in both WT and *Arom^{hum}* mice, and furthermore, it was markedly higher in *Arom^{hum}* LAM tissue than in WT LAM tissue (Fig. 4E). The stromal component in QM had negligible ER α expression (*SI Appendix, Fig. S5*). Therefore, locally produced E₂ in LAM tissues seems to be mediated via high LAM fibroblastic ER α expression, resulting in hernia formation in *Arom^{hum}* mice.

ER α -Target Gene Expression Induced by Local E₂ Excess in LAM Tissue Is Increased in *Arom^{hum}* Mice. To identify the early molecular events responsible for estrogen-induced muscle tissue fibrosis, myocyte atrophy, and hernia formation, we performed an RNA expression microarray analysis of LAM in WT and *Arom^{hum}* mice at the age of 3 wk (before the start of morphologic changes in the muscle or hernia development). Multidimensional scaling analysis of the datasets from *Arom^{hum}* and WT mice showed statistically significant differences; 92 genes were expressed preferentially in LAM of *Arom^{hum}* mice and 33 genes were preferentially expressed in WT mice (Table 1 and *Dataset S1*). Pathway analysis listed the hepatic fibrosis pathway as the first up-regulated canonical pathway, and E₂ was listed as the third upstream regulator in *Arom^{hum}* mice (Tables 2 and 3). The expression of the previously established estrogen-target gene *Greb1* was significantly higher (1.89-fold) in *Arom^{hum}* mice than in WT mice. We verified the mRNA levels of *Greb1* and several other estrogen-target genes (*Pgr*, *Ccnd1*, and *Adora1*) by real-time PCR in tissue lysates and primary fibroblasts of UAM and LAM from 3-wk-old WT and *Arom^{hum}* mice (43–46). In general,

mRNA levels of these estrogen-responsive genes tend to be higher in abdominal muscle tissues or fibroblasts with higher E₂ levels (*Arom^{hum}* vs. WT mice) and with higher ER α expression (LAM vs. UAM) (Fig. 4 F–M). Furthermore, to investigate whether ER α mediates the effects of E₂ in LAM fibroblasts, we treated LAM primary fibroblasts from WT or *Arom^{hum}* mice with E₂ in the presence or absence of the E₂/ER antagonist ICI 182780 or the ER α -selective E₂ antagonist methyl-piperidino-pyrazole (MPP). E₂ increased mRNA levels of *Pgr* and *Greb1* after 48-h of treatment. ICI 182780 or MPP inhibited the stimulatory effect of E₂ on gene expression of *Pgr* or *Greb1* (Fig. 4 N and O and *SI Appendix, Fig. S7 A, B, E, and F*). ER α knockdown significantly down-regulated mRNA levels of *Pgr* and *Greb1*, which could not be restored with E₂ treatment (Fig. 4 P and Q and *SI Appendix, Figs. S6 and S7 I and J*). These results strongly suggest that estrogen action in LAM fibroblasts of *Arom^{hum}* mice was drastically enhanced via locally produced estrogen and high ER α expression, leading to hernia formation.

The Role of Fibroblast Proliferation and Excessive ECM Formation in Estrogen-Induced Hernia Formation. Fibroblasts constitute the key cell type of the stroma and are important for wound healing and collagen formation in fibrotic tissues (47). To further determine the underlying mechanisms of locally produced estrogen in fibroblast proliferation, function, and hernia formation in LAM, K ζ 67 immunostaining (indicating cell proliferation) was performed in UAM, LAM, and QM of WT and *Arom^{hum}* mice. K ζ 67 immunoreactivity was predominantly observed in the LAM stromal component and scarcely present in myocytes of WT and

Table 2. Ingenuity pathway analysis revealed top three up-regulated canonical pathways in *Arom^{hum}* mice

Top three up-regulated canonical pathways	<i>P</i> value
Hepatic fibrosis/hepatic stellate cell activation	1.18E-04
Agranulocyte adhesion and diapedesis	1.18E-03
Parkinson's signaling	1.99E-03

Table 3. Ingenuity pathway analysis revealed top three upstream regulators in *Arom^{hum}* mice

Top three upstream regulators	P value
SOX4	3.33E-08
SRF	5.39E-07
E ₂	2.36E-06

Arom^{hum} mice. K₆₇ immunostaining, although low, could be detected in UAM stromal tissue and was negligible in the QM stromal component of both mice. The highest percentage of K₆₇⁺ nuclei was observed in LAM stromal cells of *Arom^{hum}* mice (Fig. 5A and B). Letrozole treatment strikingly decreased the number of K₆₇⁺ fibroblasts in LAM tissue of *Arom^{hum}* mice (Fig. 5C). These results show that estrogen induced-fibroblast proliferation was increased in vivo in LAM tissue of *Arom^{hum}* mice.

Primary fibroblasts isolated from LAM tissue of WT mice were treated with physiological doses of E₂ (0.1 nM to 10 nM) for 24 h; cell proliferation, indicated by proliferating cell nuclear antigen levels, and fibrosis, indicated by Col1A, were increased in proportion to the dose of estrogen (Fig. 5D). ER α protein levels were decreased after E₂ treatment, suggesting the effectiveness of the E₂ treatment. Interestingly, RNA microarray analysis of LAM of *Arom^{hum}* mice demonstrated that of the top 33 up-regulated genes, 13 are known to be involved in the fibrotic response (Table 1). The higher expression of the fibrosis-related genes *Kiss1*, *Ren1*, *Emb*, *Timp1*, *Spon2*, and *Eln* in LAM of *Arom^{hum}* compared with WT tissues was verified by real-time PCR (Fig. 5E–J). In *Arom^{hum}* mice, mRNA levels of *Kiss1*, *Ren1*, *Emb*, *Timp1*, and *Spon2* in LAM were also significantly higher compared with UAM (Fig. 5E–J). Microarray analysis showed that the fibrotic pathways were activated in LAM tissue of *Arom^{hum}* mice (Table 2). Furthermore, we treated LAM primary fibroblasts from WT or *Arom^{hum}* mice with E₂ in the presence or absence of the E₂/ER antagonist ICI 182780 or the ER α -selective E₂ antagonist MPP. E₂ increased mRNA levels of *Kiss1* and *Spon2* after a 48-h treatment. ICI 182780 or MPP inhibited the stimulatory effect of E₂ on these two fibrotic gene expressions (Fig. 5K and L and *SI Appendix*, Fig. S7C, D, G, and H). ER α knockdown significantly down-regulated mRNA levels of *Kiss1* and *Spon2* in the presence of E₂ treatment (Fig. 5M and N and *SI Appendix*, Figs. S6 and S7K and L). Together, these results demonstrated that E₂ excess and higher ER α expression induced not only fibroblast proliferation but also a sharp increase in ECM formation in LAM fibroblasts of *Arom^{hum}* mice.

***Arom^{hum}* Mice also Display Decreased Circulating T Levels and Androgen-Responsive Gene Expression.** Intriguingly, we found that circulating T levels were significantly lower in *Arom^{hum}* mice than in WT controls (Fig. 6A) and were restored to levels comparable to those in WT mice after letrozole treatment (Fig. 3D). These data suggest that elevated brain aromatase and estrogen formation in *Arom^{hum}* mice may suppress gonadotropins, leading to decreased testicular T secretion. An alternative interpretation could be that increased aromatase activity leads to T depletion via converting it into E₂. This, however, is unlikely because the roughly estimated rate of conversion of serum T to E₂ is about 0.3% in *Arom^{hum}* mice (48). T exerts its biological action via binding to the AR. Besides the full-length AR (AR-FL), mRNA levels of AR45, one of the AR variants (49), were also reported to be present in skeletal muscle tissue (50, 51). Using primers that amplify total AR (both AR-FL and AR45) in UAM and LAM tissues, we found similar levels of total AR mRNA in WT and *Arom^{hum}* mice (Fig. 6B). Using an antibody that specifically recognizes only AR-FL, AR-FL immunostaining was observed in both myocytes and stromal cells (Fig. 6C). Interestingly, using a second antibody recognizing both AR-FL and

AR45 in mouse and human for immunoblotting, both AR-FL and AR45 proteins were identified in abdominal skeletal muscle tissues (Fig. 6D). Human prostate cancer cell line LNCaP expressed both AR-FL and AR45 and served as positive controls

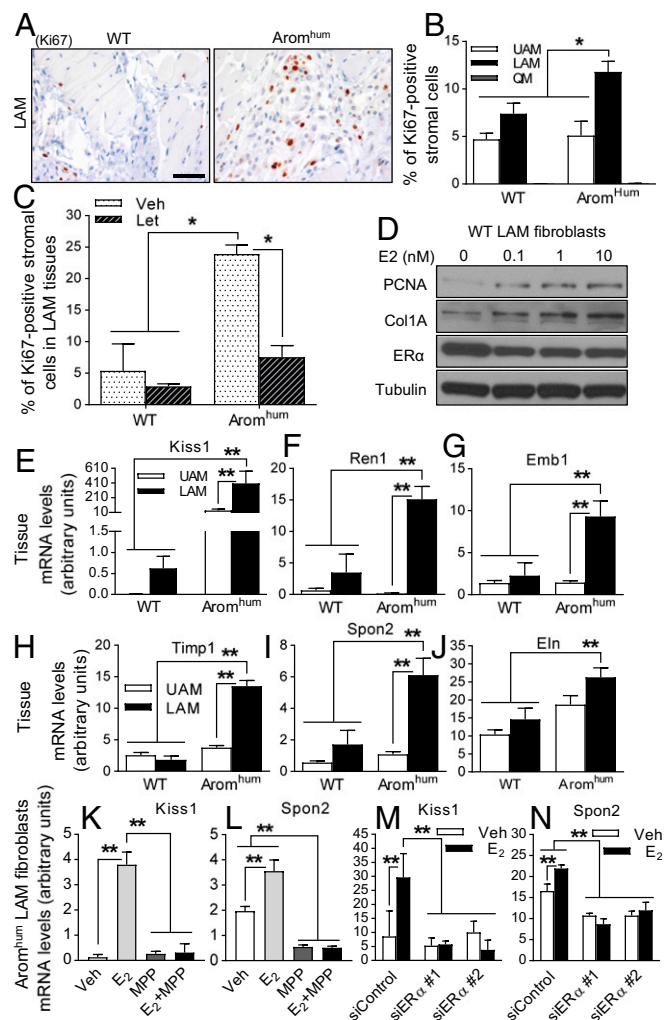


Fig. 5. Increased ER α expression and estrogen production in LAM tissue are responsible for LAM fibroblast proliferation and collagen formation in *Arom^{hum}* mice. (A) Cell proliferation indicated by K₆₇ immunoreactivity was measured in LAM tissue. (Scale bar, 50 μ m.) (B) A minimum of 1,000 nuclei were counted in sections to calculate the percent of K₆₇⁺ stromal cells in UAM, LAM, and QM of WT and *Arom^{hum}* mice. Two-way ANOVA with Sidak's multiple comparison test, **P* < 0.05, *n* = 10. (C) The effect of letrozole (Let) treatment on stromal cell proliferation determined by calculation of the percent of K₆₇⁺ nuclei in UAM and LAM of WT and *Arom^{hum}* mice treated with letrozole. Veh, vehicle. Two-way ANOVA with Tukey's multiple comparison test, **P* < 0.05, *n* = 8–11. (D) Cell proliferation marker proliferating cell nuclear antigen (PCNA) and protein levels of type I collagen (Col1A) were determined by immunoblotting in primary LAM fibroblasts of WT mice treated with the physiological doses of E₂ for 24 h. Tubulin protein levels served as the loading control. Data are representative of three independent experiments. mRNA levels of profibrotic genes *Kiss1* (E), *Ren1* (F), *Emb* (G), *Timp1* (H), *Spon2* (I), and *Eln* (J) were measured in UAM and LAM tissues of WT and *Arom^{hum}* mice at 3 wk of age. mRNA levels of *Kiss1* and *Spon2* in primary LAM fibroblasts from *Arom^{hum}* mice after MPP (10 μ M) treatment (K and L) or siRNA-mediated knockdown of ER α (M and N) in the presence or absence of E₂ (10 nM). Cells were pretreated with MPP for 2 h before the addition of E₂. Veh, vehicle. GAPDH mRNA levels served as the control. Two-way ANOVA with Tukey's multiple comparison test, **P* < 0.05, ***P* < 0.01, *n* = 10 mice in each group.

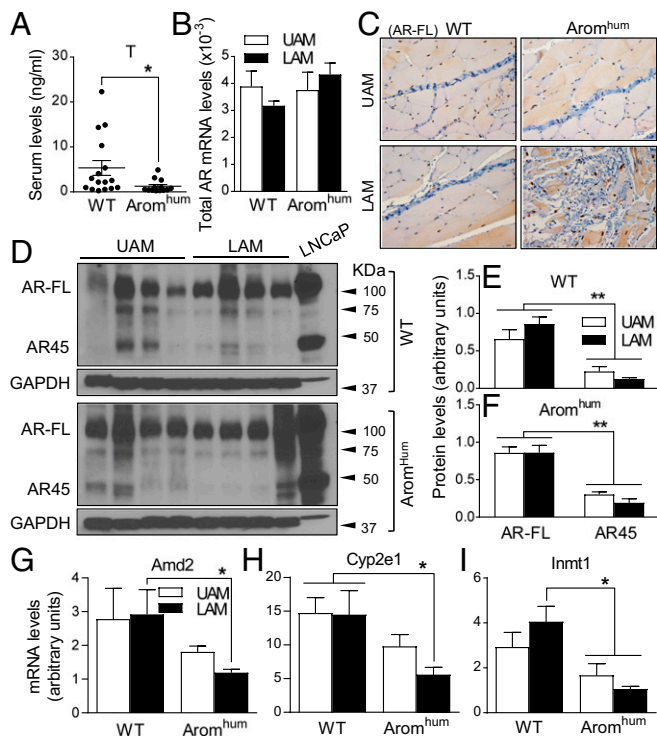


Fig. 6. Androgen action is lower in LAM of *Arom^{hum}* mice. (A) Serum T levels in WT and *Arom^{hum}* mice were measured by radioimmunoassay. Mouse sera were collected from 26-wk-old mice. Two-tailed Student's *t* test, $*P < 0.05$, $n = 15$. (B) Total AR mRNA levels (AR-FL and AR45) in UAM and LAM tissues of WT and *Arom^{hum}* mice. Two-way ANOVA with Tukey's multiple comparison test, $n = 10$. (C) Nuclear AR-FL assessed by IHC in UAM and LAM of WT and *Arom^{hum}* mice. $n = 8$. (Scale bar, 50 μ m; Magnification: C, 40 \times .) (D) AR-FL and AR45 protein levels in UAM and LAM tissues of WT and *Arom^{hum}* mice. GAPDH protein levels served as the loading control. Human prostate cancer cell line LNCaP served as AR-FL and AR45 positive controls. Quantification of AR-FL and AR45 by densitometry in UAM and LAM of WT (E) and *Arom^{hum}* (F) mice. Two-way ANOVA with Sidak's multiple comparison test, $**P < 0.01$, $n = 4$ mice in each group. mRNA levels of androgen-responsive genes *Amd2* (G), *Cyp2e1* (H), and *Inmt1* (I) in UAM and LAM tissues of WT and *Arom^{hum}* mice. GAPDH mRNA levels served as the control. Two-way ANOVA with Tukey's multiple comparison test, $*P < 0.05$, $n = 10$ mice per group.

(50, 52, 53). AR-FL protein levels were significantly higher than AR45 protein levels in all UAM and LAM tissues of both WT and *Arom^{hum}* mice (Fig. 6 D–F). However, protein levels of AR-FL and AR45 did not significantly vary between LAM and UAM in WT or *Arom^{hum}* mice (Fig. 6 D–F). Additionally, AR-FL and AR45 protein levels were not different between WT UAM and *Arom^{hum}* UAM, nor were they different between WT LAM and *Arom^{hum}* LAM (SI Appendix, Fig. S8). Overall, AR-FL seemed to be the predominant AR type in all LAM and UAM tissues examined.

Microarray analysis using LAM tissues of 3-wk-old WT and *Arom^{hum}* mice showed that 8 of the 33 genes that were significantly down-regulated in LAM of *Arom^{hum}* mice encode androgen-response proteins (Table 1 and Dataset S1). Real-time PCR verified that mRNA levels of the androgen target genes *Amd2*, *Cyp2e1*, and *Inmt1* were significantly lower in LAM of *Arom^{hum}* mice compared with LAM of WT mice (Fig. 6 G–I). In addition to higher estrogenic activity, lower androgen action in LAM tissue via low serum T levels may also contribute to hernia formation in *Arom^{hum}* mice.

Men with Inguinal Hernia Show Higher ER α Expression, Proliferative Activity, and ECM Formation in Stroma and Lower AR Expression in Myocytes in LAM Tissues. To determine whether the patterns of ER α and AR protein expression, stromal proliferation, and

ECM formation in men are comparable to those in mice, IHC for ER α , AR (using an antibody that specifically recognizes AR-FL), and K $_67$ and Masson's trichrome staining (to detect fibrosis) were performed in normal LAM tissue from hernia-free men ($n = 6$; age 50–68 y) or extended LAM tissue from men with indirect inguinal hernia ($n = 6$; age 60–77 y). Masson's trichrome staining indicated higher ECM formation and numbers of fibroblasts with myofiber atrophy in LAM of hernia patients compared with hernia-free patients (Fig. 7 A, E, and F). Similar to the mouse muscle tissue ER α expression pattern, human ER α expression was significantly higher in the stromal cells of LAM tissue from hernia patients (H-score: 29.06 ± 5.86) compared with tissues from hernia-free patients (H-score: 7.64 ± 1.59). ER α expression was negligible in myocytes (Fig. 7 B and G). AR-FL expression in LAM myocytes was significantly lower in hernia patients (H-score: 20.88 ± 2.17) than in hernia-free patients (H-score: 59.16 ± 17.39) (Fig. 7 C and H). Stromal cell proliferation indicated by K $_67$ staining was significantly increased in hernia patients (1.2%) compared with hernia-free controls (0.3%) (Fig. 7 D and I). Thus, cell-specific ER α expression pattern, cell proliferation, and fibrosis in human indirect inguinal hernia tissue are similar to those observed in the *Arom^{hum}* mouse hernia model.

Discussion

Arom^{hum} mice represent a unique and pathologically relevant experimental model to study the relationship between aromatization of androgen to estrogen, the downstream estrogenic and androgenic effects in muscle tissue, and LAM fibrosis and atrophy, leading to hernia development. Human aromatase expression driven by its alternatively used cognate promoters (I.4 and to a lesser extent PII) in *Arom^{hum}* mice resembled the human patterns of age-related increase in aromatase expression and estrogen formation in peripheral tissues, including LAM tissue, and an accompanying decrease in circulating T levels (25). Our data strongly indicate that locally produced E $_2$ acting on highly estrogen-sensitive and ER α -rich LAM fibroblasts led to stromal fibrosis, myocyte atrophy, and eventually inguinal hernia formation. The role of E $_2$ in this phenomenon is clear because the inhibition of E $_2$ production by an aromatase inhibitor prevented hernia formation. The possibly contributing roles of decreased T levels that are observed in *Arom^{hum}* mice and restored to normal with an aromatase inhibitor, however, are less clear. Decreased T levels are possibly due to increased brain E $_2$ levels via the brain expression of human aromatase, leading to decreased gonadotropin and then testicular T secretion. As the incidence of inguinal hernia and peripheral aromatase expression increase with age in men, our findings have a particular clinical significance not only for understanding the mechanisms underlying maintenance of skeletal muscle mass in various body sites, but also for assessing hernia risk and developing strategies for hernia prevention in a subset of elderly men (27–29).

Previous studies showed that postnatal systemic administration of exogenous estrogen or ubiquitous overexpression of a full-length aromatase cDNA with strikingly high circulating estrogen levels led to the formation of scrotal hernias in mice; in utero estrogen exposure was not necessary for this phenotype (9, 54). Our humanized aromatase mouse model is unique in that the estrogenic effect on LAM tissue and hernia formation are primarily mediated via local estrogen production by aromatase activity from the human *CYP19A1* (aromatase) gene expressed in the skeletal muscle tissue, with normal circulating E $_2$ levels. This model of muscle atrophy and hernia development is therefore more physiologically relevant to these common pathologies observed in a subset of elderly men.

Estrogen exerts its physiological functions by binding to its receptors ER α , ER β , and GPR30 (39–41). Studies of ER knockout mice show that ER α is primarily involved in the classic actions of estrogens (i.e., sexual differentiation, fertility, uterine

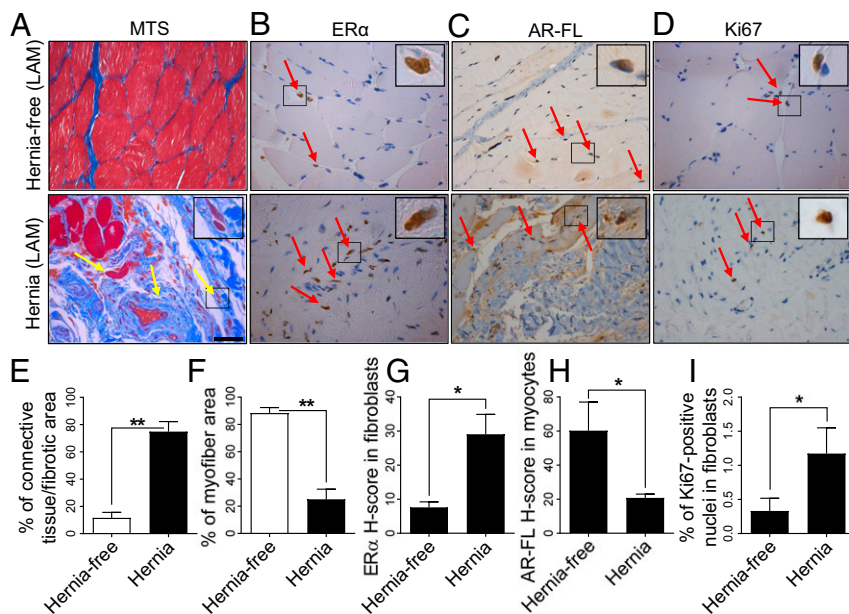


Fig. 7. (A) Masson's trichrome staining (MTS), (B) immunostaining for ER α , (C) AR-FL, and (D) Ki67 in LAM tissue from hernia-free and hernia patients. Yellow arrows indicate atrophic myocytes. Red arrows indicate brown positive staining. (Scale bar, 50 μ m; Magnification: Insets in A–D, 40 \times .) Quantification of the percentage of connective tissue or fibrotic area (E) and myofiber area (F), the average H-score (range 0–300) for ER α in fibroblasts (G) and AR-FL in myocytes (H), and the percentage of Ki67⁺ nuclei (I) in fibroblasts from hernia-free and hernia patients. Two-tailed Student's *t* test, **P* < 0.05, ***P* < 0.01, *n* = 6 per group.

function, and lactation) (39, 40). ER β has been shown to play biological roles in the central nervous system, the immune system, the ovary, and the prostate (55, 56). GPR30, on the other hand, has been linked to certain physiological and pathological effects regulated by estrogen on the central nervous, immune, renal, reproductive, and cardiovascular systems (41, 57–59). Because ER β and Gpr30 mRNA levels in LAM or UAM tissues are either barely detectable or extremely lower than ER α in our hands, the estrogenic effects on LAM fibrosis and hernia are most likely mediated primarily by ER α signaling. Indeed, we found that ER α mRNA and protein were predominantly present in the prominent perimuscular stromal fibroblast compartment of LAM tissue in both WT and *Arom*^{hum} mice. Additionally, ER α levels in LAM tissue fibroblasts were higher than those in UAM or QM tissues. Moreover, ICI 182780 (which opposes E₂ action via degradation of the ER), MPP (which is an ER α -selective E₂ antagonist), or ER α knockdown diminished estrogenic gene expression in LAM fibroblasts. Thus, we conclude that locally produced estrogen in *Arom*^{hum} LAM tissue is mediated via fibroblastic ER α , giving rise to increased stromal cell proliferation, fibrosis, muscular atrophy, and hernia development. This explains, at least in part, why atrophy and fibrosis develop in LAM tissue of *Arom*^{hum} mice, but not in other muscle groups (i.e., UAM and QM).

Gene-expression profiling allowed us to identify a number of molecular pathways and target genes activated early by E₂/ER α in LAM tissues before the hernias become manifest. These pathways include ER α -driven fibroblast activation and fibrosis pathways (44–46, 60, 61). Consistent with these findings, E₂ is found to induce fibrosis in pathologic tissues, including gynecostasia, uterine fibroid tumors, and the skin of patients with systemic sclerosis (62–64). Several known E₂/ER α target genes were highly expressed in LAM tissue of *Arom*^{hum} mice. Moreover, some of these genes, (e.g., *Greb1* and *Pgr*) were selectively induced in primary fibroblasts of LAM tissue, suggesting that these effects took place primarily in the fibroblast compartment of LAM tissue. *Greb1* is a chromatin-bound ER coactivator and is essential for ER-mediated transcription (61). *Greb1* is also one

of the most highly estrogen-inducible genes and correlates well with changes in ER activity following breast cancer treatment (43, 65). Thus, *Greb1* may also contribute to fibroblast proliferation in LAM. Moreover, the estrogen-responsive fibrotic genes, including *Kiss1*, *Krt8*, *Krt7*, *Spon2*, *Krt18*, *Tnc*, *Plod2*, and *Eln*, were also increased in LAM of *Arom*^{hum} mice (Table 1), as has been reported for several other tissues (66–72). On the other hand, several other well-known estrogen response genes (e.g., *Adora1*, *Tff1*, and *Susd3*) were not induced by aromatase expression in LAM tissue (44, 45, 73), suggesting epigenetic differences between tissues or cell types may account for E₂/ER α induction of a select group of genes.

T is the major substrate of the aromatase enzyme. T is not only converted by aromatase to E₂ in target tissues for estrogenic action, but is also converted by 5 α -reductatase-1 or -2 into a potent and nonaromatizable androgen, DHT (74). mRNA levels of 5 α -reductase-1 or -2 were undetectable or barely detectable in LAM tissue. Thus, in LAM, androgen action must be provided primarily via an interaction of T with AR. In fact, in double

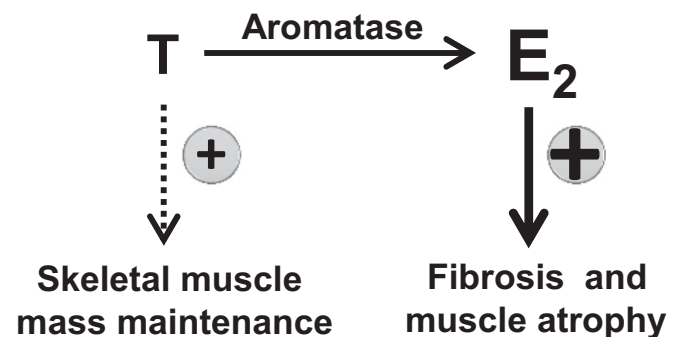


Fig. 8. Schematic demonstrating the effect of a shift from androgen to estrogen action induced by human aromatase gene expression in LAM tissue on fibrosis, myocyte atrophy, and hernia formation in mice.

5 α -reductase knockout mice (for both types 1 and 2), T was shown to exert androgenic action via AR (74).

T and AR exert anabolic effects on skeletal muscle, resulting in muscle protein synthesis and increased muscle mass (75, 76). Overall, AR-FL seems to be the predominant AR type in both LAM and UAM tissue, suggesting a more important role of AR-FL in both WT and *Arom^{hum}* LAM tissues. The precise role of AR45 in abdominal muscle tissue, however, needs further investigation. We also found that serum T was significantly lower in *Arom^{hum}* mice, which may contribute to decreased androgen action. These results indicate that low circulating T levels, together with local estrogen excess, shift the steroid balance from androgen to estrogen in *Arom^{hum}* mice or in a subset of elderly men, leading to muscle atrophy and hernia, possibly via decreased muscle mass.

In summary, the lower portion of the LAM tissue adjacent to the scrotal opening is particularly enriched with ER α -expressing fibroblasts and thus sensitive to E₂. Expression of aromatase in mice, which directly converts circulating T to E₂ locally in the muscle or in the brain, leads to stromal proliferation, muscle atrophy, and hernia development in LAM tissue via up-regulation of estrogenic action and down-regulation of androgenic action (Fig. 8). All *Arom^{hum}* mice uniformly developed fibrosis, myocyte atrophy, and hernia, which was entirely blocked and prevented by an aromatase inhibitor. There are currently no experimental or approved medical options for the prevention of inguinal hernias associated with skeletal muscle fibrosis and atrophy in a subset of men. In particular, the surgical repair of a recurrent hernia is quite problematic and carries a high risk of treatment failure or recurrence. Intriguingly, our findings uncover a previously unrecognized mechanism for LAM fibrosis and atrophy and inguinal hernia formation and open new horizons for drug development to prevent hernia, especially recurrent hernia after surgery in vulnerable populations, such as elderly men. Currently available aromatase inhibitors or analogs of androgen may provide alternative or complementary management modalities in addition to surgical repair.

Materials and Methods

***Arom^{hum}* Mouse Maintenance, Hernia Assessment, and Letrozole Treatment.** The *Arom^{hum}* mouse (FVB/N background) was generated and genotyped in our laboratory, as previously described (34). *Arom^{hum}* transgenic mice contain the complete human aromatase coding region, a >75-kb promoter region including promoters I.4, I.7, I.f, I.6, I.3 and PII, and the 3'-polyadenylation site. Mice were maintained on a 14-h light:10-h dark cycle with standard chow (7912; Harlan Teklad) and water available ad libitum. All animal experiments were approved by and conducted in accordance with guidelines established by the Institutional Animal Care and Use Committee at Northwestern University. Animals were randomly used for all experiments in a blinded manner. Hernia development in 32 *Arom^{hum}* male mice was monitored by weekly visual inspection and palpation from 3 to 26 wk of age. Age-matched WT male littermates were used as controls. Hernia dimensions were measured using a digital caliper, and hernia area was calculated by the formula, area (mm²) = length (mm) \times width (mm). At the designated endpoints, UAM, LAM, and QM from each individual mouse were resected, with one-half of the tissue snap-frozen in liquid nitrogen, and the other half fixed in 4% phosphate-buffered paraformaldehyde for histological and IHC analyses. All tissue and serum samples were collected from mice between 10:00 AM and 12:00 PM (noon) to avoid possible variability in daily hormone fluctuations. In some experiments, male mice were randomly treated with letrozole (10 μ g/d per mouse) using 90-d continuous-release pellets (Innovative Research of America) or control pellets starting at 3 wk of age (77).

Pellets were implanted subcutaneously on the lateral side of the neck between the ear and the shoulder.

Human Subjects. We recruited six hernia-free men (aged 50–68 y) and six men with hernias (aged 60–77 y) from the First Affiliated Hospital of Nanjing Medical University in China. Men were excluded if they had chronic debilitating disease, had undergone chemotherapy or radiation therapy, or had received any hormonal treatments within the past 3 mo. Muscle biopsy specimens from the inguinal area were obtained and preserved in 10% formalin and embedded in paraffin. The human study was approved by the Medical Ethics Committee of the First Affiliated Hospital of Nanjing Medical University and complied strictly with the national ethical guidelines of China. Written informed consent was obtained from all participants before inclusion in the study. All participants were identified by assigned numbers.

Primary Mouse Skeletal Muscle Tissue Fibroblast Culture, Hormonal Treatments, and Small-Interfering RNA Knockdown. Isolation and culture of primary skeletal muscle tissue fibroblasts were performed based on a modified version of an established protocol for culturing human or mouse adipose fibroblasts and mouse skeletal myoblasts (78–80). In brief, UAM and LAM tissues from six WT and six *Arom^{hum}* mice were minced and digested with collagenase D (1.5 U/mL), dispase II (2.4 U/mL), and CaCl₂ (2.5 mM) at 37 °C for 30–60 min. Single-cell suspensions were prepared by filtration through a 75- μ m sieve. Fibroblasts in cell suspensions were allowed to attach collagen-coated Petri dishes for 15 min and unattached myoblasts were removed. Primary fibroblasts were obtained by growing cells in DMEM/F-12 medium with 10% FBS. Under such conditions, there was preferential growth of fibroblastic cells which comprised 99% of the total population within 2 wk (80). Cells were grown to 80% confluence and placed in serum-free and phenol-free medium for 16 h before treatment. Primary fibroblasts were incubated in serum-free and phenol-free DMEM/F-12 in the absence or presence of physiological doses of E₂ (0.1 nM, 1 nM, and 10 nM; Sigma-Aldrich) for 24–48 h. Cells were pretreated with ICI 182780 (100 nM) or MPP (10 μ M) for 2 h before the addition of E₂. Cell extracts were prepared for real-time RT-PCR analysis or immunoblotting. To knock down endogenous ER α expression, primary fibroblasts were transfected with two separate ON-TARGETplus mouse ER α siRNAs (Dharmacon) using DharmaFECT 1 transfection reagent (Dharmacon) for 48 h. ON-TARGETplus nontargeting control siRNA (Dharmacon) was transfected as a negative control.

Data Availability. The RNA microarray data that support the findings of this study have been deposited to the National Center for Biotechnology Information Gene Expression Omnibus database under the accession no. GSE92748 (<https://www.ncbi.nlm.nih.gov/geo/>).

Statistical Analysis. Results are expressed as mean \pm SEM, unless otherwise indicated. Statistically significant differences at $P < 0.05$ were determined using two-tailed Student's *t* test, one-way ANOVA, or two-way ANOVA. All statistical tests were performed using the GraphPad Prism software.

Extended method and information about RNA isolation and quantitative real-time PCR, exon-specific RT-PCR amplification, histology, Masson's trichrome staining, IHC, scoring of immunoreactivity, protein extraction and immunoblotting, serum and tissue hormone levels, and microarrays, and data analyses are described in *SI Appendix, Materials and Methods*.

ACKNOWLEDGMENTS. We thank Dr. Elizabeth M. McNally, Dr. Pin Yin, Dr. Alexis R. Demonbreun, Dr. Matthew J. Schipma, and Dr. Matthew T. Dyson at Northwestern University for all their help and insight; the Ligand Assay & Analysis Core at the University of Virginia Center for Research in Reproduction for measuring serum sex steroid hormones and gonadotrophins; the Mouse Histology & Phenotyping Laboratory and the Pathology Core Facility Laboratories at Northwestern University for performing immunohistochemistry; and Dean Evans from Novartis for providing the aromatase inhibitor letrozole. This work was supported by the NIH Grant R37-HD36891 (to S.E.B.).

- Chung L, Norrie J, O'Dwyer PJ (2011) Long-term follow-up of patients with a painless inguinal hernia from a randomized clinical trial. *Br J Surg* 98:596–599.
- Rutkow IM (2003) Demographic and socioeconomic aspects of hernia repair in the United States in 2003. *Surg Clin North Am* 83:1045–1051, v–vi.
- Matthews RD, Neumayer L (2008) Inguinal hernia in the 21st century: An evidence-based review. *Curr Probl Surg* 45:261–312.
- Bay-Nielsen M, Perkins FM, Kehlet H; Danish Hernia Database (2001) Pain and functional impairment 1 year after inguinal herniorrhaphy: A nationwide questionnaire study. *Ann Surg* 233:1–7.
- Malangoni MA, Rosen MJ (2008) *Hernias. Sabiston Textbook of Surgery: The Biological Basis of Modern Surgical Practice*, eds Townsend C, Beauchamp RD, Evers BM, Mattox K (Saunders Elsevier, Philadelphia), 20th Ed, pp 1092–1119.
- Matthews RD, et al.; Veterans Affairs Cooperative 456 Studies Program Investigators (2007) Factors associated with postoperative complications and hernia recurrence for patients undergoing inguinal hernia repair: A report from the VA Cooperative Hernia Study Group. *Am J Surg* 194:611–617.
- Yang B, Jiang ZP, Li YR, Zong Z, Chen S (2015) Long-term outcome for open preperitoneal mesh repair of recurrent inguinal hernia. *Int J Surg* 19:134–136.

8. Gardner WU (1936) Sexual dimorphism of the pelvis of the mouse, the effect of estrogenic hormones upon the pelvis and upon the development of scrotal hernias. *Am J Anat* 59:459–483.
9. Hazary S, Gardner WU (1960) Influence of sex hormones on abdominal musculature and the formation of inguinal and scrotal hernias in mice. *Anat Rec* 136:437–443.
10. Bjorn JC, Gardner WU (1956) Inguinal hernias in female mice treated with androgens or bearing grafts of testes. *Endocrinology* 59:48–54.
11. Amato G, et al. (2013) Histological findings in direct inguinal hernia: Investigating the histological changes of the herniated groin looking forward to ascertain the pathogenesis of hernia disease. *Hernia* 17:757–763.
12. Amato G, et al. (2012) Muscle degeneration in inguinal hernia specimens. *Hernia* 16: 327–331.
13. Amato G, et al. (2009) Histological findings of the internal inguinal ring in patients having indirect inguinal hernia. *Hernia* 13:259–262.
14. Gunnarsson U, Degerman M, Davidsson A, Heuman R (1999) Is elective hernia repair worthwhile in old patients? *Eur J Surg* 165:326–332.
15. Kingsnorth A, LeBlanc K (2003) Hernias: Inguinal and incisional. *Lancet* 362: 1561–1571.
16. Zendejas B, et al. (2013) Incidence of inguinal hernia repairs in Olmsted County, MN: A population-based study. *Ann Surg* 257:520–526.
17. Goh VH, Tong TY, Mok HP, Said B (2007) Interactions among age, adiposity, body-weight, lifestyle factors and sex steroid hormones in healthy Singaporean Chinese men. *Asian J Androl* 9:611–621.
18. Jasuja GK, et al. (2013) Age trends in estradiol and estrone levels measured using liquid chromatography tandem mass spectrometry in community-dwelling men of the Framingham Heart Study. *J Gerontol A Biol Sci Med Sci* 68:733–740.
19. Li JY, et al. (2005) Decline of serum levels of free testosterone in aging healthy Chinese men. *Aging Male* 8:203–206.
20. Gray A, Feldman HA, McKinlay JB, Longcope C (1991) Age, disease, and changing sex hormone levels in middle-aged men: Results of the Massachusetts Male Aging Study. *J Clin Endocrinol Metab* 73:1016–1025.
21. Leifke E, et al. (2000) Age-related changes of serum sex hormones, insulin-like growth factor-1 and sex-hormone binding globulin levels in men: Cross-sectional data from a healthy male cohort. *Clin Endocrinol (Oxf)* 53:689–695.
22. Ferrini RL, Barrett-Connor E (1998) Sex hormones and age: A cross-sectional study of testosterone and estradiol and their bioavailable fractions in community-dwelling men. *Am J Epidemiol* 147:750–754.
23. Simon D, et al. (1992) The influence of aging on plasma sex hormones in men: The Telecom Study. *Am J Epidemiol* 135:783–791.
24. Orwoll E, et al. (2006) Testosterone and estradiol among older men. *J Clin Endocrinol Metab* 91:1336–1344.
25. Larionov AA, et al. (2003) Aromatase in skeletal muscle. *J Steroid Biochem Mol Biol* 84:485–492.
26. Matsumine H, Hirato K, Yanaihara T, Tamada T, Yoshida M (1986) Aromatization by skeletal muscle. *J Clin Endocrinol Metab* 63:717–720.
27. Bulun SE, Simpson ER (1994) Competitive reverse transcription-polymerase chain reaction analysis indicates that levels of aromatase cytochrome P450 transcripts in adipose tissue of buttocks, thighs, and abdomen of women increase with advancing age. *J Clin Endocrinol Metab* 78:428–432.
28. Cleland WH, Mendelson CR, Simpson ER (1985) Effects of aging and obesity on aromatase activity of human adipose cells. *J Clin Endocrinol Metab* 60:174–177.
29. Hemsell DL, Grodin JM, Brenner PF, Siiteri PK, MacDonald PC (1974) Plasma precursors of estrogen. II. Correlation of the extent of conversion of plasma androstenedione to estrone with age. *J Clin Endocrinol Metab* 38:476–479.
30. Burrows H (1934) The occurrence of scrotal hernia in mice under treatment with oestrin. *Br J Surg* 21:507–512.
31. Rohrmann S, et al. (2011) The prevalence of low sex steroid hormone concentrations in men in the Third National Health and Nutrition Examination Survey (NHANES III). *Clin Endocrinol (Oxf)* 75:232–239.
32. Shores MM, Matsumoto AM (2014) Testosterone, aging and survival: Biomarker or deficiency. *Curr Opin Endocrinol Diabetes Obes* 21:209–216.
33. Shores MM, Matsumoto AM, Sloan KL, Kivlahan DR (2006) Low serum testosterone and mortality in male veterans. *Arch Intern Med* 166:1660–1665.
34. Zhao H, et al. (2012) A humanized pattern of aromatase expression is associated with mammary hyperplasia in mice. *Endocrinology* 153:2701–2713.
35. Stocco C (2012) Tissue physiology and pathology of aromatase. *Steroids* 77:27–35.
36. Harada N, Utsumi T, Takagi Y (1993) Tissue-specific expression of the human aromatase cytochrome P-450 gene by alternative use of multiple exons 1 and promoters, and switching of tissue-specific exons 1 in carcinogenesis. *Proc Natl Acad Sci USA* 90:11312–11316.
37. Brodie A, Inkster S, Yue W (2001) Aromatase expression in the human male. *Mol Cell Endocrinol* 178:23–28.
38. Simpson ER (2009) Sex, fat and breast cancer. *Gynecol Endocrinol* 25:1.
39. Kregel JH, et al. (1998) Generation and reproductive phenotypes of mice lacking estrogen receptor beta. *Proc Natl Acad Sci USA* 95:15677–15682.
40. Lubahn DB, et al. (1993) Alteration of reproductive function but not prenatal sexual development after insertional disruption of the mouse estrogen receptor gene. *Proc Natl Acad Sci USA* 90:11162–11166.
41. Olde B, Leeb-Lundberg LM (2009) GPR30/GPER1: Searching for a role in estrogen physiology. *Trends Endocrinol Metab* 20:409–416.
42. Feder D, et al. (2013) Hormonal receptors in skeletal muscles of dystrophic mdx mice. *BioMed Res Int* 2013:604635.
43. Dunbier AK, et al. (2010) Relationship between plasma estradiol levels and estrogen-responsive gene expression in estrogen receptor-positive breast cancer in postmenopausal women. *J Clin Oncol* 28:1161–1167.
44. Lin Z, et al. (2010) Adenosine A1 receptor, a target and regulator of estrogen receptor/alpha action, mediates the proliferative effects of estradiol in breast cancer. *Oncogene* 29:1114–1122.
45. Moy I, et al. (2015) Estrogen-dependent sushi domain containing 3 regulates cytoskeleton organization and migration in breast cancer cells. *Oncogene* 34:323–333.
46. Castro-Rivera E, Samudio I, Safe S (2001) Estrogen regulation of cyclin D1 gene expression in ZR-75 breast cancer cells involves multiple enhancer elements. *J Biol Chem* 276:30853–30861.
47. Ivano M, et al. (2002) Evidence that fibroblasts derive from epithelium during tissue fibrosis. *J Clin Invest* 110:341–350.
48. Shozu M, et al. (2003) Estrogen excess associated with novel gain-of-function mutations affecting the aromatase gene. *N Engl J Med* 348:1855–1865.
49. Lu C, Luo J (2013) Decoding the androgen receptor splice variants. *Transl Androl Urol* 2:178–186.
50. Ahrens-Fath I, Politz O, Geserick C, Haendler B (2005) Androgen receptor function is modulated by the tissue-specific AR45 variant. *FEBS J* 272:74–84.
51. Weiss B, Faus H, Haendler B (2007) Phylogenetic conservation of the androgen receptor AR45 variant form in placental mammals. *Gene* 399:105–111.
52. Hu DG, et al. (2014) Identification of androgen receptor splice variant transcripts in breast cancer cell lines and human tissues. *Horm Cancer* 5:61–71.
53. Mitani Y, et al. (2014) Alterations associated with androgen receptor gene activation in salivary duct carcinoma of both sexes: Potential therapeutic ramifications. *Clin Cancer Res* 20:6570–6581.
54. Li X, et al. (2001) Altered structure and function of reproductive organs in transgenic male mice overexpressing human aromatase. *Endocrinology* 142:2435–2442.
55. Weihua Z, et al. (2003) Update on estrogen signaling. *FEBS Lett* 546:17–24.
56. Younes M, Honma N (2011) Estrogen receptor β . *Arch Pathol Lab Med* 135:63–66.
57. Filardo EJ, Thomas P (2012) Minireview: G protein-coupled estrogen receptor-1, GPER-1: Its mechanism of action and role in female reproductive cancer, renal and vascular physiology. *Endocrinology* 153:2953–2962.
58. Hsu I, Vitkus S, Da J, Yeh S (2013) Role of oestrogen receptors in bladder cancer development. *Nat Rev Urol* 10:317–326.
59. Prossnitz ER, Barton M (2011) The G-protein-coupled estrogen receptor GPER in health and disease. *Nat Rev Endocrinol* 7:715–726.
60. Bonéy-Montoya J, Ziegler YS, Curtis CD, Montoya JA, Nardulli AM (2010) Long-range transcriptional control of progesterone receptor gene expression. *Mol Endocrinol* 24: 346–358.
61. Mohammed H, et al. (2013) Endogenous purification reveals GREB1 as a key estrogen receptor regulatory factor. *Cell Rep* 3:342–349.
62. Agarwal VR, et al. (1998) Molecular basis of severe gynecomastia associated with aromatase expression in a fibrolamellar hepatocellular carcinoma. *J Clin Endocrinol Metab* 83:1797–1800.
63. Aida-Yasuoka K, et al. (2013) Estradiol promotes the development of a fibrotic phenotype and is increased in the serum of patients with systemic sclerosis. *Arthritis Res Ther* 15:R10.
64. Luo N, et al. (2014) Estrogen-mediated activation of fibroblasts and its effects on the fibroid cell proliferation. *Transl Res* 163:232–241.
65. Ng CW, et al. (2013) Extensive changes in DNA methylation are associated with expression of mutant huntingtin. *Proc Natl Acad Sci USA* 110:2354–2359.
66. Gopaul R, Knaggs HE, Lephart ED (2012) Biochemical investigation and gene analysis of equol: A plant and soy-derived isoflavonoid with antiaging and antioxidant properties with potential human skin applications. *Biofactors* 38:44–52.
67. Shah YM, Basrur V, Rowan BG (2004) Selective estrogen receptor modulator regulated proteins in endometrial cancer cells. *Mol Cell Endocrinol* 219:127–139.
68. Stephens SB, Chahal N, Munaganuru N, Parra RA, Kauffman AS (2016) Estrogen stimulation of Kiss1 expression in the medial amygdala involves estrogen receptor- α but not estrogen receptor- β . *Endocrinology* 157:4021–4031.
69. Tan O, Ornek T, Seval Y, Sati L, Arici A (2008) Tenascin is highly expressed in endometriosis and its expression is upregulated by estrogen. *Fertil Steril* 89:1082–1089.
70. Tan S, et al. (2014) Identification of miR-26 as a key mediator of estrogen stimulated cell proliferation by targeting CHD1, GREB1 and KPN2B. *Breast Cancer Res* 16:R40.
71. Walker G, et al. (2007) Estrogen-regulated gene expression predicts response to endocrine therapy in patients with ovarian cancer. *Gynecol Oncol* 106:461–468.
72. Chung D, Gao F, Jegga AG, Das SK (2015) Estrogen mediated epithelial proliferation in the uterus is directed by stromal Fgf10 and Bmp8a. *Mol Cell Endocrinol* 400:48–60.
73. Prest SJ, May FE, Westley BR (2002) The estrogen-regulated protein, TFF1, stimulates migration of human breast cancer cells. *FASEB J* 16:592–594.
74. Mahendroo MS, Cala KM, Hess DL, Russell DW (2001) Unexpected virilization in male mice lacking steroid 5 alpha-reductase enzymes. *Endocrinology* 142:4652–4662.
75. de Rooy C, Grossmann M, Zajac JD, Cheung AS (2016) Targeting muscle signaling pathways to minimize adverse effects of androgen deprivation. *Endocr Relat Cancer* 23:R15–R26.
76. Pihlajamaa P, Sahu B, Jänne OA (2015) Determinants of receptor- and tissue-specific actions in androgen signaling. *Endocr Rev* 36:357–384.
77. Long BJ, et al. (2004) Therapeutic strategies using the aromatase inhibitor letrozole and tamoxifen in a breast cancer model. *J Natl Cancer Inst* 96:456–465.
78. Chen D, et al. (2007) Prostaglandin E2 induces breast cancer related aromatase promoters via activation of p38 and c-Jun NH(2)-terminal kinase in adipose fibroblasts. *Cancer Res* 67:8914–8922.
79. Zhao H, et al. (2009) A novel promoter controls Cyp19a1 gene expression in mouse adipose tissue. *Reprod Biol Endocrinol* 7:37.
80. Rando TA, Blau HM (1994) Primary mouse myoblast purification, characterization, and transplantation for cell-mediated gene therapy. *J Cell Biol* 125:1275–1287.